© 2020. Published by The Company of Biologists Ltd | Journal of Cell Science (2020) 133, jcs253260. doi:10.1242/jcs.253260

PUBLISHER'S NOTE

Expression of Concern: Mechanisms underlying p53 regulation of *PIK3CA* transcription in ovarian surface epithelium and in ovarian cancer

Arezoo Astanehe, David Arenillas, Wyeth W. Wasserman, Peter C. K. Leung, Sandra E. Dunn, Barry R. Davies, Gordon B. Mills and Nelly Auersperg

This Expression of Concern relates to *J. Cell Sci.* (2008) **121**, 664-674 (doi:10.1242/jcs.013029)

A reader informed the journal that there were several potential issues with the blots in this paper, which were also highlighted on the PubPeer website. Possible band duplications were highlighted in: p21 and actin blots in OSE457 and MCF7 panels in Fig. 1A; actin blots in A2780 and OVCAR5 panels in Fig. 1B; actin blots in IOSE 166 h and WI38 panels in Fig. 2A; T-AKT blot in IOSE 166a panel in Fig. 3A; T-AKT blots in OSEC2 and IOSE166a panels in Fig. 3B.

Journal of Cell Science contacted Dr Auersperg, the corresponding author, to request the original blots, but unfortunately the blots were no longer available. As is our standard practice in such cases, without the original full blots to support the results shown in these figures, the journal referred the matter to the Vice-President, Research and Innovation at The University of British Columbia (UBC), asking them to provide further information and a recommendation as to the next steps.

As part of the case summary provided to UBC, the journal included a visual demonstration of the similarities between the blots in question using the open-source software 'Forensically'. It is important to note that the software was not used to detect similarities between blots, but rather to highlight them.

UBC contacted the journal upon conclusion of its investigation and stated that no misconduct had occurred. The journal requested the report to understand how the committee arrived at this conclusion, stating that we would have expected the report to comment on the soundness of the conclusions in the paper. UBC provided the report, which showed that the committee had focused its investigation on the use of the Forensically software tool. The report concluded that "…there is no basis for concluding that the blots in question were duplicated or improperly altered." Their recommendation was: "Care should be taken whenever a report of duplication has resulted from analysis using the current version of the Forensically software." Furthermore, UBC stated: "It is not the University's place to comment on [the soundness and trustworthiness of the data] – we leave those determinations to the expertise of peer reviewers, editorial boards and the academic community more generally."

The journal clarified that Forensically was not used to detect any potential duplications, and reiterated its expectations that an institutional investigation would indeed comment on the validity of the data, highlighting relevant sections from the COPE (Committee on Publication Ethics) website; Journal of Cell Science and its publisher, The Company of Biologists, are members of COPE. The journal requested that UBC conduct a more-detailed investigation into the issues raised about this paper, but UBC declined.

The journal therefore referred the matter to an external expert, requesting an opinion on the soundness of the conclusions of the paper by Astanahe et al., considering that the blots in question are unreliable. Our expert advisor expressed the opinion that the conclusions are possibly still sound, noting two additional papers published subsequently that report results similar to those of the paper in question.

The journal also contacted all of the co-authors of the paper, and although there was some initial correspondence, further attempts to communicate with them went unanswered.

The journal is therefore publishing this Expression of Concern to make readers aware of these issues and our efforts to resolve them.

Journal of Cell Science

irradiation. Contrary to the data from Stambolic et al. (Stambolic et al., 2001), who observed no change in PTEN levels using human colorectal carcinoma cells with mutated p53, the PTEN levels in OVCAR3 also increased, suggesting that the regulation of PTEN levels occurs by different means in the two lines and is p53-independent at least in OVCAR3 cells.

To determine whether the decrease in p110α protein levels was p53 dependent, the effect of expression of wild-type p53 on p110α protein levels was examined. Table 1 lists the p53 status and known average copy numbers of *PIK3CA* of the cancer lines based on fluorescent in situ hybridization or comparative genomic hybridization. Infection of p53 decreased p110α protein levels compared with uninfected and GFP-infected controls in all lines, regardless of p53 status (Fig. 1B). Therefore, in the presence of wild-type or mutant p53, expression of additional wild-type p53 is sufficient to decrease p110α levels in ovarian cancer cells.

We examined the effect of p53 on p110α expression using temperature-sensitive (ts) cells. Western blot analysis demonstrated overexpression of p53 at 34°C, indicating binding of SV40 large T antigen (TAg) to p53, stabilization of p53 and a resultant lack of p53 function. After the switch in temperature to 39°C, p53 levels decreased and p53 became functional, as indicated by increases in p21 protein levels (Fig. 2A). p110α levels were highest at 34°C, decreased significantly after 1 day at 39°C and were hardly detectable after 5 days (Fig. 2A). Moreover, consistent with Stambolic et al. (Stambolic et al., 2001), PTEN levels in ts cells increased, although modestly, at 39°C. These studies show that p53 is a major regulator of p110α protein levels, with more modest effects on PTEN. Importantly, the effects are inverse, with p53 decreasing p110α while increasing PTEN levels, which should result in additive inhibitory effects on the PI3K/AKT-*P*/PTEN pathway.

p53 negatively regulates *PIK3CA* transcript levels

Real-time quantitative reverse transcriptase (RT)-PCR showed that *PIK3CA* transcript levels in the ts cells OSEC2, non-tumorigenic immortalized human ovarian surface epithelial cells (IOSE) 166h and IOSE 166a were highest at 34°C (Fig. 2B). Upon gain in p53 function after a single day at 39°C, *PIK3CA* transcript levels decreased and remained low over 5 days at 39°C. This decrease was not due to crowding or reduced cell proliferation because OSEC2 maintained at 34°C for 5 days acquired significantly higher *PIK3CA* transcript levels. Diminished *PIK3CA* transcripts were reversible when cells were shifted from 39 to 34°C (data not shown). At 39°C, the *PIK3CA* transcript levels of the non-ts control cells IOSE 80pc, IOSE 397 and WI38 were dramatically increased, ruling out the effect of temperature alone as a cause of the decline in transcripts in the ts cells.

p53 negatively regulates PI3K activity

In the ts OSEC2, IOSE 166h and IOSE 166a cells, phosphorylated AKT (AKT-*P*) levels increased with serum stimulation but, at 39°C, the increase in AKT-*P* levels was considerably less than at 34°C. Thus, in the presence of functional p53, PI3K-dependent AKT phosphorylation decreased in parallel with decreased levels of p110α (Fig. 3A). Similarly, all three ts cell lines, when stimulated with varying concentrations of fetal bovine serum (FBS), showed increased AKT-*P* levels with higher serum stimulation at both 34°C and 39°C, with higher degrees of increase at 34°C than at 39°C (data not shown). In IOSE 397 and WI38 control cells, AKT-*P* levels increased at 39°C, therefore ruling out the possibility that the observed effect was due to temperature alone (data not shown). Also,

Fig. 2. Conditional activation of p53 causes a decrease in p110α protein and *PIK3CA* transcript levels. (A) Western blot analyses of ts OSEC2, IOSE 166h and IOSE 166a cells show that, after a switch from 34 to 39°C, p53 became functional, p21 and PTEN levels increased, whereas p110α levels decreased. IOSE lines with non-functional p53 (IOSE 80pc and IOSE 397) and WI38 cells with wild-type p53 were used as controls to rule out direct effects of temperature on p110α levels. There was no decrease in p110α levels with the increase in temperature in these non-ts control cells. WI38 cells expressed low levels of p110α protein; these levels did not change in response to increased temperature. Furthermore, in the control cells, PTEN levels remained unchanged (IOSE 80pc) or decreased (IOSE 397 and WI38) at 39°C. +/– indicate functional/non-functional SV40 TAg or p53. (B) Real-time quantitative RT-PCR of the cells shown in A demonstrates that, upon temperature shift to 39°C, which results in p53 activation, *PIK3CA* transcript levels significantly decreased in the ts lines (OSEC2, IOSE 166h, IOSE 166a). *PIK3CA* transcript levels increased at 39°C in non-ts control cells (IOSE 80pc, IOSE 397 and WI38). At 34°C, at which p53 remained inactive, all the ts cell lines had higher *PIK3CA* transcript levels on day 5 at 34°C compared to day 1 at 34°C. The expression level of the ribosomal RNA gene was used as control.

LY294002 treatment blocked phosphorylation of AKT at both temperatures in all cell lines, demonstrating that the response was PI3K dependent (data not shown). The effect of p53 on AKT-*P* was further studied in OSEC2, IOSE 166h and IOSE 166a cells on days 1 and 3 after the shift from 34 to 39°C with either serum stimulation (10%) or serum starvation (0.5%) (Fig. 3B). At 39°C, AKT-*P* levels were significantly lower after serum stimulation compared to those at 34°C, whereas total AKT (T-AKT) levels did not change (Fig. 3B). In IOSE 397 and WI38 controls, AKT-*P* levels did not decrease, but rather increased with the shift to 39°C (data not shown). Thus,

Journal of Cell Science

western blot analysis for AKT-*P* showed decreased PI3K activity concomitant with gain in p53 function and decrease in p110α levels.

For a more direct evaluation of PI3K activity, an AKT-PH-GFP construct was transiently transfected into OSEC2, IOSE 166h and IOSE 166a cells at 34°C. Membrane localization of the GFP tag indicates localization of the AKT PH domain (AKT-PH) to the membrane, providing a surrogate assessment of PI3K (and PTEN) activity. Fig. 4A illustrates the five different preparations tested for OSEC2 cells. After serum stimulation, OSEC2 cells at 34°C exhibited brightly stained spots, indicating strong membrane localization of AKT-PH-GFP (Fig. 4A). In comparison, AKT-PH-GFP was not targeted to the membrane at 39°C. Thus, serum stimulation induced significantly less membrane localization in the OSEC2 cells at 39°C. In OSEC2 cells treated with LY294002, only weak membrane localization was detected, demonstrating that this response is PI3K dependent (Fig. 4A). Similar results were obtained using the IOSE 166h and IOSE 166a cells under all the above conditions, although Fig. 4B,C only illustrate the serum-stimulated preparations at both 34 and 39°C in IOSE 166h and IOSE 166a cells, respectively. In summary, the percentage of cells with strong membrane localization was significantly higher in stimulated compared with serum-starved ts cells at 34°C and, more importantly, compared to ts cells at 39°C with or without serum stimulation (Fig. 4D), indicating reduced PI3K activity in the presence of functional p53. IOSE 397 and WI38 control cells did not show the same reduction in membrane localization at 39°C upon serum stimulation that was observed in the ts cells (data not shown).

Decrease in proliferation upon gain in p53 function

We investigated the effect of gain in p53 function on proliferation. Ki-67 is highly expressed in cycling cells and absent in G0. After only 1 day at 39°C there was a significant reduction of Ki-67-positive nuclei in OSEC2 cells (Fig. 5A) and, after 5 days, there was almost no proliferation. By contrast, Ki-67 levels in controls either increased (IOSE 397) or did not change (WI38) in response to a shift from 34 to 39°C.

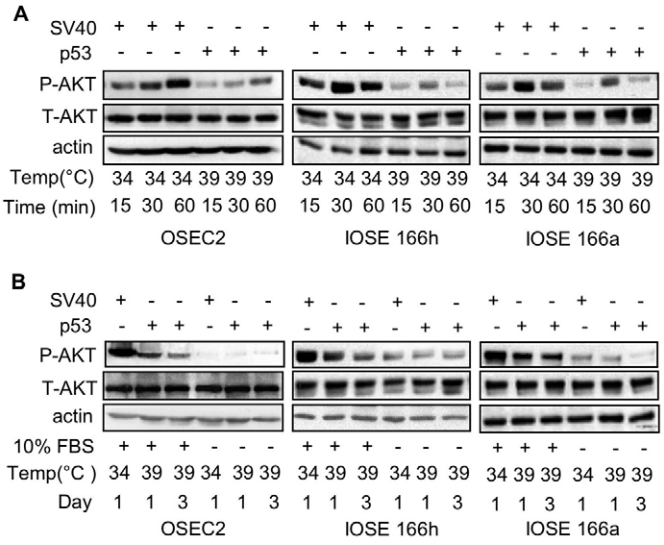

Fig. 3. Conditional activation of p53 causes a decline in PI3K activity. (A) Western blot analyses demonstrate maximum AKT phosphorylation in OSEC2 cells after 60 minutes, and in IOSE 166h and IOSE 166a cells after 30 minutes, of stimulation with 10% FBS following serum starvation (0.5% FBS). Phosphorylated AKT (P-AKT) levels were lower at 39°C compared with at 34°C. (B) Western blots of OSEC2, IOSE 166h and IOSE 166a cells show that AKT-*P* levels decreased after a shift to 39°C, whereas total AKT (T-AKT) levels remained unchanged.

Increase in apoptosis upon gain in p53 function

A quantitative ELISA-based assay showed that levels of apoptosis were significantly higher in OSEC2 cells at 39°C compared to at 34°C. Apoptosis also increased in OSEC2 cells at 34°C treated with LY294002 (Fig. 5B). The ability of LY294002 to induce apoptosis in these cells in which p53 is inactive strongly argues for a contribution of the PI3K pathway in maintaining viability regardless of the presence or absence of functional p53. IOSE 397 and WI38 cells showed similar levels of apoptosis at 34 and 39°C, suggesting that the increased apoptosis at 39°C was due to gain in p53 function. In addition, by nuclear morphology, OSEC2 cells demonstrated significantly more apoptotic figures at 39°C than at 34°C (data not shown).

Identification of two alternate exon 1 sequences in *PIK3CA*

The promoter region of *PIK3CA* has not been previously characterized. In order to identify the *PIK3CA* promoter, we first sought to identify the transcription start site. Approximately 60% of human promoters are located proximal to CpG islands (Gardiner-Garden and Frommer, 1987). Annotations from the UCSC genome browser indicate the presence of a CpG island 50,473 base pairs (bp) upstream of the translation start site [coordinates, chr3:180,348,768-180,399,240 (human genome assembly 17)], and a putative first exon 50,227 bp upstream of the currently annotated first exon [coordinates, chr3:180,349,013-180,399,240 (human genome assembly 17)]. The combination of transcript data and the CpG island suggested a possible location for the *PIK3CA* promoter.

The rapid amplification of cDNA ends (5′ RACE) technique was used to confirm the presence of the putative upstream first exon and to determine the transcript 5′ untranslated region (5′ UTR). The tailed OSEC2 sample was PCR amplified with GSP2 and AAP (abridged amplification primer). A subsequent nested amplification with GSP3 and AUAP (abridged universal amplification primer) on 1:100 dilution of the PCR product obtained in the first PCR resulted in a single band, approximately 500 bp in length (Fig. 6A). This band was gel purified and sequenced. The sequence obtained was aligned against the *PIK3CA* sequence on the UCSC genome browser using the BLAT alignment software. This identified the presence of a new exon, which we called exon1a, upstream of the current first exon, which we now refer to as exon2(1). Exon1a is 50,579 bp upstream of exon2(1) [coordinates, chr3:180,348,661-180,399,240 (human genome assembly 17)] (Fig. 6C). The sequencing of the RACE band demonstrated that exon1a splices directly to exon2(1) (Fig. 6D).

Interestingly, the sequence obtained from the RACE product was different from the sequence predicted to be an upstream exon based on RefSeq genes. However, with RACE analysis, we were unable to detect this potential exon using the primers specific to the tail portion of the cDNA, perhaps because of the high GC content of this region. However, using internal forward primer (GSP5) and GSP3, the presence of this GC-rich upstream exon was confirmed (Fig. 6B). We refer to this exon, which is in agreement with the RefSeq gene exon prediction, as exon1b. This PCR product was gel purified and sequenced, which demonstrated that exon1b splices directly into exon2(1) (Fig. 6B). Exon1b is 50,227 bp upstream of exon2(1) [coordinates, chr3:180,349,013-180,399,240 (human genome assembly 17)] (Fig. 6C). Analysis of the splice junctions of exons1a, 1b and 2(1) determined the presence of consensus splice

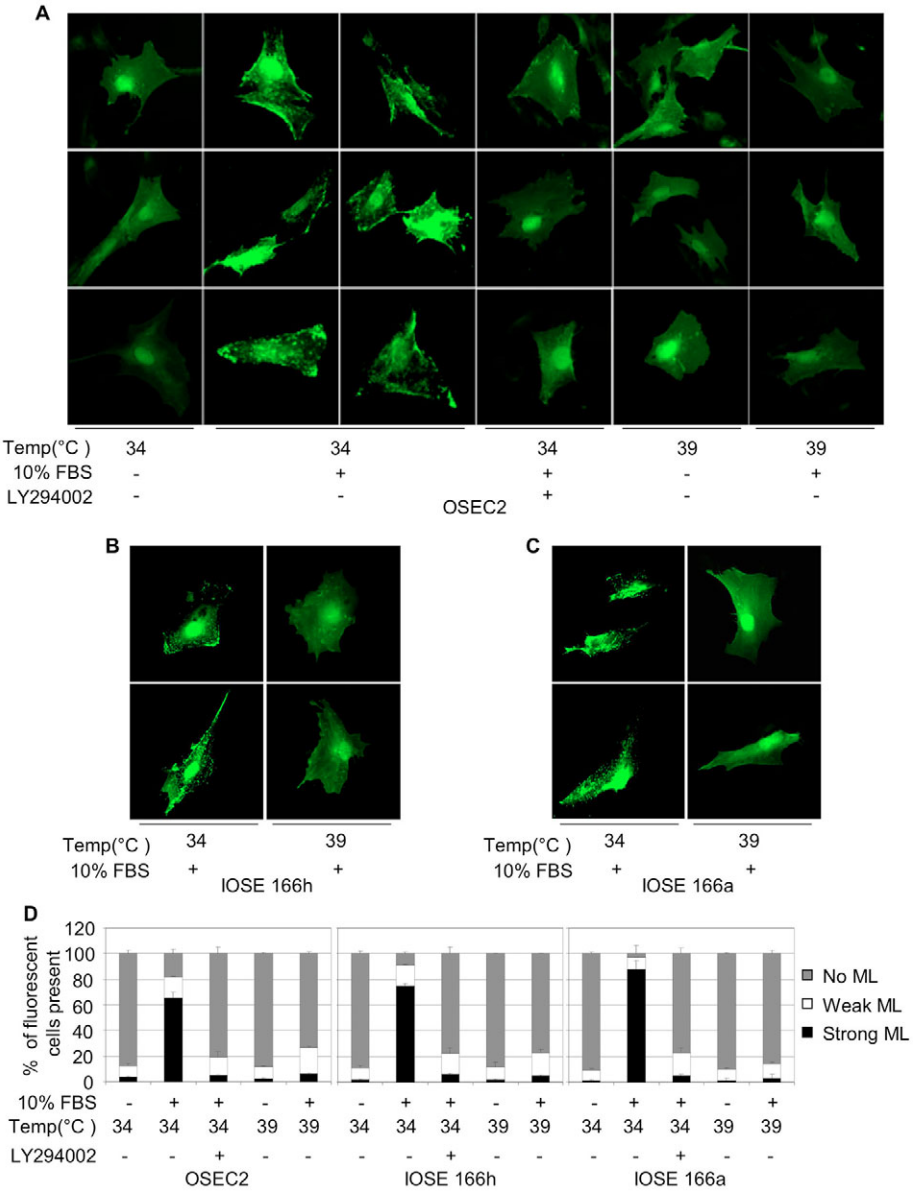

Fig. 4. Conditional activation of p53 causes a reduction in AKT membrane localization. (A) OSEC2 cells at 34°C in the absence of serum stimulation did not show membrane localization of AKT-PH-GFP protein. Upon serum stimulation (10% FBS) at 34°C, the AKT-PH-GFP protein was targeted to the membrane, indicative of increased PI3K activity in the absence of functional p53. When serum-stimulated OSEC2 cells at 34°C were treated with 20 μM of the PI3K inhibitor LY294002 for 1 hour, membrane localization was minimal. OSEC2 cells with functional p53 at 39°C did not demonstrate membrane localization in either the absence or presence of serum stimulation. Similar to the OSEC2 cells, IOSE 166h (B) and IOSE 166a (C) cells showed a significant reduction in AKT-PH-GFP membrane localization at 39°C compared with at 34°C after serum stimulation. (D) Between 300 and 400 cells per group in each cell line (OSEC2, IOSE 166h and IOSE 166a) in the preparations shown in A, B and C were grouped by percentage into three categories: strong, weak and no membrane localization (ML). Only with serum stimulation at 34°C was there a highly significant increase in the percentage of cells with strong membrane localization (P<0.001). Statistical analysis was by one-way ANOVA test (Tukey).

sites at the 3′ ends of exons1a and 1b, and at the 5′ end of exon2(1). Moreover, splice analysis of both exon1a and exon1b determined that these exons do not have splice junctions on their 5′ ends, indicating that they are two alternate first exons (Fig. 4D).

p53 binds directly to a putative *PIK3CA* promoter

Bioinformatics analysis identified candidate p53 target sequences in the promoter of *PIK3CA* (Fig. 6E). As shown in Fig. 6E, there are five clusters of predicted p53 half-sites within promoter1a and two clusters within promoter1b; these half-sites are separated by 0-13 bp. A list of p53-binding sites is provided in supplementary material Table S1.

Binding of p53 to *PIK3CA* was shown by chromatin immunoprecipitation (ChIP; Fig. 7A). OSEC2 cells at 39°C showed the presence of bands in regions 1a1, 1a2, 1a3 and 1a4 within promoter1a. There was no band detected in any region of promoter1b. At 34°C, ChIP analysis identified bands in regions 1a2 and 1a3. The presence of bands in regions 1a2 and 1a3 at both temperatures suggests that, at 34°C, not all of p53 is inactivated by TAg. Furthermore, at 34°C, there were no bands detected in promoter regions 1a1 and 1a4, indicating the specificity of the assay.

All the putative p53-binding sites (Fig. 6E) within promoter1a (sites 1-5) that demonstrated binding in the ChIP assay were investigated using electrophoretic mobility shift assay (EMSA) and the corresponding EMSA oligonucleotides. Oligo4 demonstrated the strongest binding-affinity for p53 out of the five oligonucleotides tested (data not shown). We therefore focused on oligo4 for the remainder of the studies. Both recombinant p53 protein (Fig. 7Ba) and OSEC2 nuclear lysates at 39°C (Fig. 7Bb) showed binding of p53 to oligo4, whereas there was no binding with OSEC2 nuclear lysates at 34°C. There was significant loss of p53 binding with unlabeled competition. EMSA using the mutated form of oligo4 (harboring point mutations at the core CnnG site) showed significantly reduced binding to p53, and the unlabeled mutated oligo4 had a decreased ability to compete for binding to p53 compared with wild-type oligo4 (Fig. 7B). Moreover, a supershift

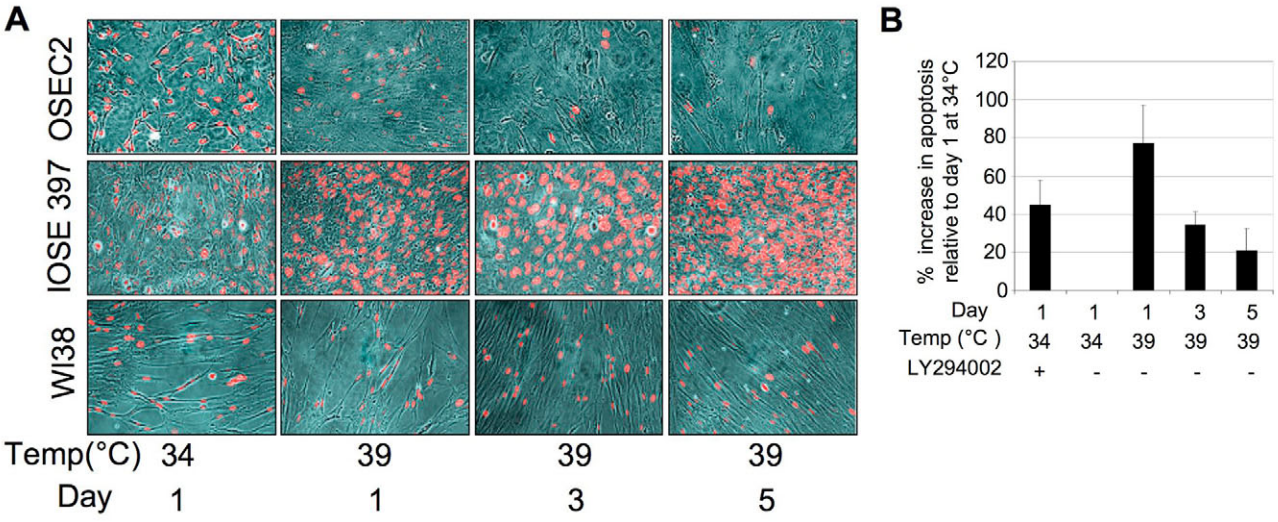

Fig. 5. Conditional activation of p53 causes decreased proliferation and increased apoptosis. (A) Ki-67 immunofluorescence of OSEC2 cells demonstrates that, on day 1, OSEC2 cells at 34°C had many positively stained nuclei (red), whereas OSEC2 cells at 39°C had decreased numbers of Ki-67-positive nuclei and, thus, had decreased proliferation. Ki-67 staining of non-ts IOSE 397 and WI38 cells did not show the same pattern: with the switch in temperature from 34 to 39°C, the number of Ki-67-positive nuclei in the IOSE 397 cultures increased, whereas the number of positive nuclei in WI38 cells remained unchanged. (B) Cell death detection ELISA to quantify levels of apoptosis of the cells demonstrated that the percentage of apoptotic OSEC2 cells at 39°C was significantly higher than at 34°C. Treatment of cells at 34°C with LY294002 also resulted in increased apoptosis.

was observed with the use of p53 antibody (Fig. 7Bb). These results indicate that the *PIK3CA*-promoter-derived oligonucleotide specifically binds p53. EMSA using A2780 (wild-type p53) and SKOV3 (p53 null) nuclear lysates showed similar results to OSEC2 nuclear lysates (data not shown).

p53 binding represses promoter1a of *PIK3CA*

To determine whether the p53-binding site in the *PIK3CA* promoter contributes to transcription regulation, promoter1a with either a wild-type or mutated oligo4 region was cloned into a pGL3 luciferase construct. Fig. 7C shows that there was approximately an 83% decrease in activity of *PIK3CA* pGL3-P1A construct at 39°C in the presence of functional p53 compared with the promoter activity at 34°C. Thus, p53 represses the activity of *PIK3CA* promoter1a. In addition, the mutated form of the construct (pGL3-P1A-mut4) showed less than 50% decrease in promoter activity at 39°C. Therefore, changing the core (CnnG) nucleotides of the p53-binding site significantly reduces *PIK3CA* promoter activity, suggesting that the integrity of the p53-binding site in the *PIK3CA* promoter plays a role in its repression by p53.

Discussion

Epithelial ovarian carcinomas (EOC) are characterized by a high incidence of p53 inactivation and increased PI3K activity (Schlosshauer et al., 2003; Shayesteh et al., 1999). Using IOSE lines, in which p53 expression can be regulated via temperature shifts, as well as ovarian carcinoma lines, we identified and characterized, for the first time, the *PIK3CA* promoter and two of its transcriptional start sites, and demonstrated that this promoter is negatively regulated by direct binding of p53. Assays of the influence of p53 on promoter function directly, and on cell proliferation and apoptosis, demonstrated that the degree of promoter downregulation achieved by the temperature shifts and consequent p53 activation used in this study was physiologically relevant.

The temperature shift to 39°C, which inactivates the mutated SV40 TAg, resulted in p53 that was functionally active, as indicated by the regulation of p21 levels. Our demonstration that gain in p53 function decreases p110α protein levels in ovarian carcinoma cells parallels the results reported by Singh et al. (Singh et al., 2002), who found a similar link between *PIK3CA* expression and p53 levels in upper aerodigestive tract and colon carcinoma lines. In these studies, the basis for such a link was not defined. Therefore, we investigated the molecular mechanisms underlying such interactions and found in the present study that they depend on direct binding of p53 to the *PIK3CA* promoter. In addition, we found that this interaction of p53 and *PIK3CA* also occurs in non-tumorigenic cells and therefore is not limited to malignant cells, indicating that it is a general mechanism that regulates other functions of these two mediators. We identified a specific p53-binding site within *PIK3CA* promoter1a and demonstrated the importance of this binding site for p53-dependent *PIK3CA* transrepression. The reporter assay using the mutated *PIK3CA* promoter demonstrated partial suppression upon p53 activation compared with the wild-type *PIK3CA* promoter, suggesting the presence of other functional p53-binding sites within promoter1a or activity of additional transcriptional factors involved in regulation of *PIK3CA* promoter activity. Our characterization of the promoter will facilitate future studies of *PIK3CA* transcriptional regulation.

Overexpression of wild-type p53 in ovarian cancer cells with normal or inactivated p53, even in cells with *PIK3CA* amplification, resulted in decreased p110α levels. Therefore, loss of p53 function might be one of the mechanisms that contribute to the characteristically increased p110α levels in ovarian cancer. Our results suggest that p53 inactivation results in increases of *PIK3CA* transcripts beyond those that result from amplification of 3q26 alone. The combined effects of *PIK3CA* amplification and loss of p53-mediated regulation of p110α and PTEN levels must contribute significantly to the increased signaling through the PI3K pathway. This is probably of marked functional consequences given the effects of activation of the PI3K pathway on tumor pathophysiology as well as response to therapy (Fraser et al., 2003b; Hu et al., 2002; Yuan et al., 2003).

Journal of Cell Science

Journal of Cell Science

Amplification of *PIK3CA* and p53 mutations appear to be early events in ovarian cancer development (Schlosshauer et al., 2003; Shayesteh et al., 1999). Amplification of *PIK3CA* in cells with an intact p53 pathway does not interfere with DNA-damage signals that induce p53-mediated apoptosis (Lengauer et al., 1998), whereas the increased PI3K activity in cells that lack p53 function might contribute to cell survival and accumulation of additional genomic abnormalities. Therefore, coordinate action of p53 mutation and subsequent PI3K activation, with increased genetic instability due to the loss of p53 and increased cell survival action due to PI3K activation, might contribute to the ability of cells to survive genomic stress and to develop resistance to chemotherapeutic agents (Fraser et al., 2003a).

Our characterization of the *PIK3CA* promoter and the demonstration of two alternate first exons in the 5′ UTR pave the way for future studies. The presence of transcripts that differ only in their 5′ UTR has been described for many genes (Arrick et al., 1994; Brown et al., 1999; Hempel et al., 2004; Savitsky et al., 1997; Sobczak and Krzyzosiak, 2002). This occurrence has mostly been interpreted as an evolutionary gain for refined transcriptional and translational control (Duga et al., 1999). These studies provide evidence that, because of the length and sequence of the mRNA upstream of AUG, secondary structures can occur, which will block ribosome scanning and result in varying promoter activity and translational efficiency (Meric and Hunt, 2002). The translation efficiency of eukaryotic mRNAs might vary considerably depending on the properties of their 5′ UTRs. Statistically, 5′ UTRs of low-expression mRNAs are longer and their GC content is higher (Kochetov et al., 1998). *BRCA1* is a specific example of a gene with

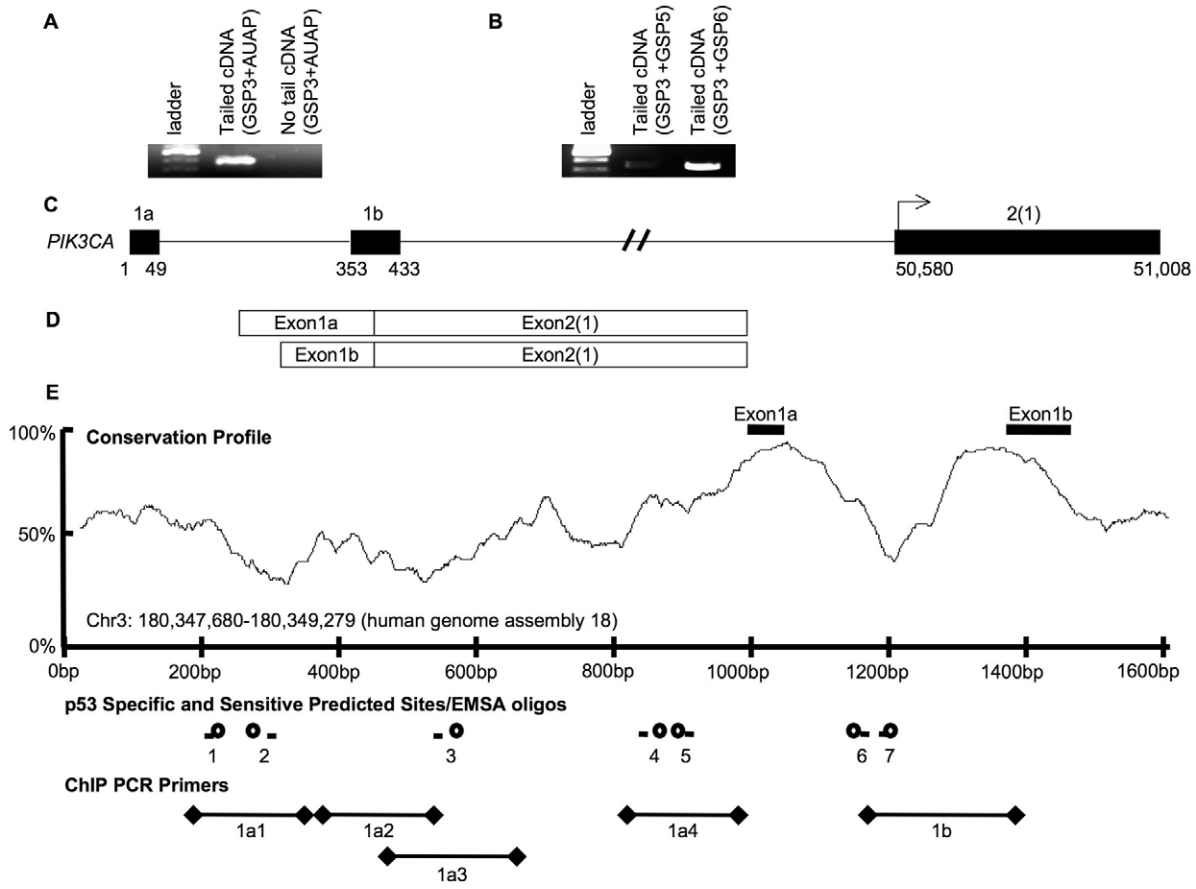

Fig. 6. Identification of two alternate upstream *PIK3CA* exons. 5′ RACE analysis was used to determine the presence of upstream exons. (A) A 1:100 dilution of the primary PCR product of the tailed cDNA was amplified with GSP3 and AUAP primers, demonstrating the presence of a single band of approximately 500 bp in size. The diluted PCR product of no tail cDNA amplified with GSP3 and AUAP was the negative control. (B) The presence of putative exon1b was confirmed using a 1:100 dilution of the primary PCR product of the tailed cDNA amplified with GSP3 and GSP5, resulting in a 442 bp band. GSP3 binds to exon2(1), whereas GSP6 and GSP5 bind to exons1a and 1b, respectively. GSP3 and GSP6 were used as positive control (429 bp) to amplify the newly identified exon1a. (C) A diagram of the first three exons of *PIK3CA* showing the nucleotide positions of the newly identified exons 1a and 1b, thereby demonstrating their nucleotide distance from exon2(1). The first nucleotide of exon1a is marked as 1 and the positions of the first and last nucleotides of the first three exons [1a, 1b and 2(1)] are accordingly labeled. The exons are indicated by the black boxes labeled 1a, 1b and 2(1); the introns are indicated by the horizontal lines connecting them. Exon2(1) [coordinates, chr3:180,399,240-180,399,668 (human genome assembly 17)] contains the translational start site (arrow). Exon1a [coordinates, chr3:180,348,661-180,348,709 (human genome assembly 17)] is in the 5′ UTR and is 50,579 bp upstream of exon2(1). Exon1b [coordinates, chr3:180,349,013-180,349,093 (human genome assembly 17)] is also in the 5′ UTR and is 50,227 bp upstream of exon2(1). Exon1a and exon1b are highly conserved, and their first nucleotides are 352 bp apart. (D) A diagram showing that there are two alternate *PIK3CA* transcripts. Exons 1a and 1b splice alternatively to exon2(1). (E) Phylogenetic footprinting and p53-binding-site analysis of promoter-proximal sequences. p53 interacts with DNA through binding to two tandem copies of a well-defined half-site. The *PIK3CA* promoter region was analyzed with two half-site filters to predict candidate binding sites. The specific profile (lines) requires the presence of two nucleotides at critical positions within the recognition sequence (CnnG). Because empirical observation suggests that some bonafide p53 target sequences diverge from the constrain in one of the two half-sites, the sensitive profile (circles) requires only one perfect match to the core sequences. The locations of the oligonucleotides used in mobility shift assays and the amplified PCR products from the ChIP experiments are indicated.

Journal of Cell Science

alternate mRNA transcripts. Similarly to *PIK3CA* (this study), *BRCA1* has two alternate first exons, and two alternate promoters upstream that produce these alternate transcripts (Xu et al., 1997). For *BRCA1*, the longer mRNA transcript that also has a higher GC content forms a stable secondary structure, which inhibits efficient translation resulting in lower levels of the protein (Sobczak and Krzyzosiak, 2002). The *PIK3CA* mRNA transcript containing exon1b (mRNA1b) is longer and has a higher GC content compared with the transcript containing exon1a. If *PIK3CA* is similar to the other genes that contain more than one 5′ UTR, then it is possible that the *PIK3CA* transcript 1b can also form secondary structures and result in less-efficient translation compared with transcript 1a. Our studies provide evidence for p53 binding to promoter1a, but not to promoter1b. This leads to the hypothesis that, in normal cells, p53 binds to regions on promoter1a and suppresses transcription starting from this promoter, whereas mRNA1b, with possible lower translation efficiency, maintains basal levels of p110α. In the absence of functional p53 protein, the suppression of promoter1a is removed and transcription can begin from promoter1a, giving rise to higher levels of mRNA1a with possible higher translational efficiency. This might provide one explanation for the increased p110α levels in ovarian cancers.

In conclusion, in conditionally immortalized OSE cells, gain in p53 function resulted in a significant downregulation of *PIK3CA* transcript levels, p110α protein levels and PI3K activity. This is the first characterization of a *PIK3CA* promoter, which will greatly facilitate further studies of PI3K action. It is also the first demonstration of a direct functional and physical interaction between p53 and *PIK3CA* in both malignant and non-malignant ovarian cells. Thus, our studies suggest a unique mechanism whereby direct binding of the p53 homotetramer to the *PIK3CA* promoter decreases *PIK3CA* transcript levels (Fig. 8). The results reveal a novel molecular mechanism by which loss of p53 function might accelerate ovarian epithelial neoplastic progression, and a potential therapeutic approach to p53 mutant ovarian cancers. The observation that such direct interactions between p53 and *PIK3CA* also occur in non-tumorigenic cells suggests that they represent a general regulatory mechanism of normal physiologic processes.

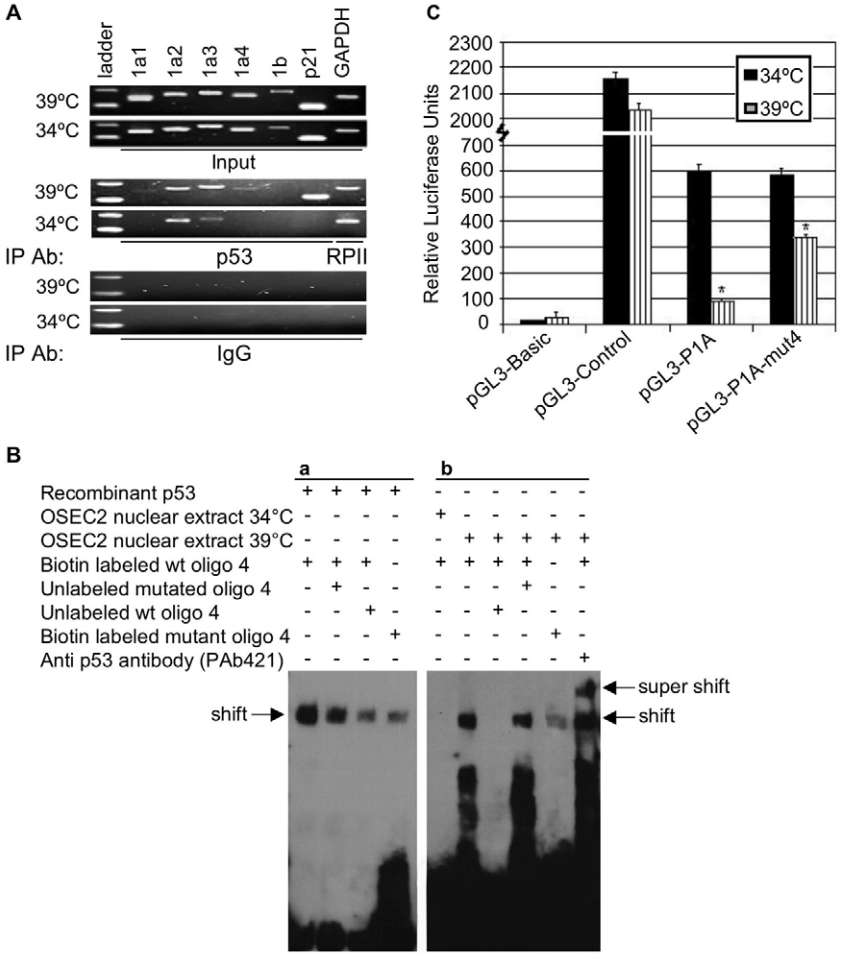

Fig. 7. p53 binds to the *PIK3CA* promoter and suppresses its activity. (A) ChIP results for OSEC2 cells. Antibodies used for immunoprecipitation (IP) are indicated below the panels. OSEC2 cells at 34°C have reduced p53 activity, whereas the cells at 39°C have full activity. PCR amplification with GAPDH primers of samples immunoprecipitated with RNA polymerase II antibody is presented as a positive control. Input DNA acts as control for levels of DNA present in each sample. Amplification with primers around the known p53-binding sites on the p21 promoter were used as positive controls. (Ba) An electrophoretically retarded complex (shift) was formed with recombinant p53 and biotin-labeled oligo4. Formation of this complex was inhibited with an excess of unlabeled wild-type oligo4. However, the unlabeled mutant oligo4, with point mutations in the core (CnnG) binding region, did not compete with the biotin-labeled oligo4 to the same extent. In addition, the biotin-labeled mutant oligo4 showed reduced interaction with p53 compared to wild-type oligo4. (Bb) Similarly to the recombinant p53, the use of nuclear lysates from OSEC2 cells at 39°C with p53 resulted in the formation of an electrophoretically retarded complex, which was competed with excess unlabeled wild-type oligo4. Similarly, the unlabeled mutant oligo4 did not compete with the biotin-labeled oligo4 to the same extent; and the biotin-labeled mutant oligo4 showed reduced interaction with p53 compared with the wild-type oligo4. The use of nuclear lysates from OSEC2 cells at 34°C without p53 did not lead to formation of an electrophoretically retarded complex (shift). Addition of an anti-p53 antibody (PAb421) to the reaction mixture induced a supershift of the protein-DNA complex, indicating the specificity of oligonucleotide for p53. (C) OSEC2 cells transfected transiently with promoter1a construct (pGL3-P1A) showed 83% less luminescence (*PIK3CA*-promoter activity) at 39°C compared with at 34°C. pGL3-P1A-mut4 construct showed significantly less decrease in promoter activity after the switch in temperature to 39°C (less than 50% decrease). pGL3-control was used as positive control and pGL3-basic was used as negative control. The values presented were normalized with the internal control (phRL-TK).

Materials and Methods

Cell lines and culture

See Table 2 for cell lines and cultures. OSE is the source of ovarian carcinomas (Auersperg et al., 2001). The limited proliferative potential of human OSE in culture can be extended by introduction of SV40 TAg (Maines-Bandiera et al., 1992), which inactivates p53 and pRb. TAg inhibits transcriptional activity of p53 by binding to its DNA-binding domain (Pipas and Levine, 2001). We created a series of ts cell lines by infecting normal OSE cells, which contain wild-type p53, with ts SV40 TAg A209, a chimeric virus containing an origin-defective adenovirus plus a ts SV40 TAg with a mutation at amino acid residue 209 (Chou, 1989; Leung et al., 2001). At 34°C, the permissive temperature, ts TAg, like wild-type TAg, binds to p53 and inactivates it. This leads to post-translational stabilization and overexpression of the inactive p53, which allows for its detection by western blot analysis. At 39°C, the non-permissive temperature, ts TAg no longer binds p53 and thus p53 levels and activity revert to normal. Using this construct, we created two ts-SV40-TAg-expressing OSE lines with extended life spans, IOSE 166a and IOSE 166h,

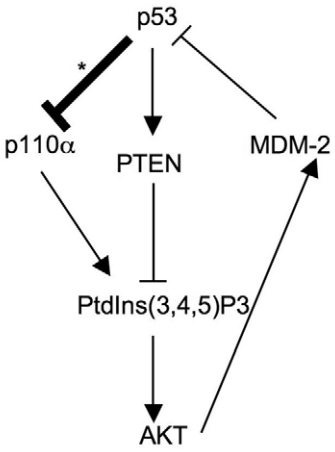

Fig. 8. The p53 and PI3K pathways regulate one another. p53 positively regulates PTEN levels, which reverse PI3K action by dephosphorylating PtdIns(3,4,5)P_3 (Stambolic et al., 2001). Our contribution to this figure is in bold with an asterisk: this study demonstrates that p53 directly regulates *PIK3CA* transcription, resulting in decreased p110α and thus PtdIns(3,4,5)P_3 levels. PtdIns(3,4,5)P_3 recruits AKT to the membrane, where AKT becomes phosphorylated and activated. In turn, activated AKT phosphorylates MDM2, which leads to the nuclear import of MDM2. In the nucleus, MDM2 binds to and degrades p53 (Zhou et al., 2001).

and line OSEC2, which expresses telomerase in addition to ts SV40T Ag and is thus a permanent line at 34°C (Davies et al., 2003). The lines IOSE 397 and IOSE 80pc were immortalized with wild-type SV40 TAg and lack functional p53 at both temperatures. The ovarian cancer lines SKOV3, OVCAR3 (ATCC, Manassas, VA), CaOV3, OVCAR5, OVCAR8 and A2780 (from T. Hamilton, Fox Chase Cancer Center, Philadelphia, PA), and the MCF7 breast cancer line were used to compare neoplastic lines with wild-type p53 to neoplastic lines with loss-of-function mutations of p53 (Table 1). The cancer cells were maintained in a 1:1 mixture of 199:105 medium (Sigma, Oakville, ON, Canada) with 5% FBS (Hyclone, Logan, UT) and the non-cancer cells in 199:105 medium with 10% FBS.

Determination of protein levels by western blots

70% confluent cultures were maintained at 34°C or moved to 39°C. Controls were maintained at 37°C. On days 1, 3 and 5, cells at 34, 37 and 39°C were lysed (PBS, pH 7.4, 1% Triton X-100, 0.5% sodium deoxycholate, 0.1% SDS containing protease inhibitor cocktail) (Sigma), and 20 μg aliquots of protein were resolved by SDS-PAGE. Antibodies were obtained from Cell Signaling Technologies (Danvers, MA): anti-p110α polyclonal rabbit antibody (no. 4254), anti-p53 mouse mAb (1C12), anti-phospho-AKT (Ser473) rabbit mAb (193H12), anti-total-AKT polyclonal rabbit antibody (no. 9272) and anti-PTEN rabbit mAb (138G6). The anti-p21 (H-164) polyclonal rabbit antibody and anti-actin (C-11) polyclonal goat antibody were from Santa Cruz Biotechnology (Santa Cruz, CA).

Determination of *PIK3CA* transcript levels by quantitative RT-PCR

At about 70% confluence, cells were placed at 34°C or moved to 39°C. Cells were lysed and the RNA isolated using the RNeasy mini kit (Qiagen, Mississauga, ON, Canada) at various time points. Genomic DNA was digested with deoxyribonuclease I, amplification grade (Invitrogen, Burlington, ON) and cDNA was synthesized using first-strand cDNA synthesis kit (Amersham Biosciences, Baie d'Urfe, QB, Canada) using random hexamers as primers. For quantitative RT-PCR, TaqMan Universal Master Mix (Applied Biosystems, Streetsville, ON, Canada) was used according to the manufacturer's instructions. The TaqMan gene expression assay for human PI3K, p110α (*PIK3CA*) (Applied Biosystems, HS00180679), containing appropriate primers and probes, was used with a GeneAmp 5700 sequence detector (Applied Biosystems).

PI3K activity

At 70% confluence, cells were moved to 39°C or maintained at 34°C. Their response to serum stimulation was studied by serum starvation in 199:105 medium with 0.5% FBS for 16 hours, followed by stimulation for 1 hour with medium containing either 0.5, 1, 5, 10 or 15% FBS. In addition, groups of cells at both 34°C and 39°C were treated with 20 μM of LY294002 (Biomol Research Laboratories, Plymouth Meeting, PA) for 1 hour prior to serum stimulation. Cells were lysed and prepared for western blot analysis. Time-dependent responses to serum were determined by serum starvation with 0.5% FBS for 16 hours, stimulation with 10% FBS for 15, 30 and 60 minutes, and subsequent western blot analysis of AKT-*P* levels. In addition, a group of cells was maintained at 34°C and another at 39°C. The cells were serum starved as explained above and either stimulated with 10% FBS for 30-60 minutes, depending on the cells being studied, or maintained with 0.5% FBS and subsequently lysed at various time points.

The AKT-PH-GFP construct contains the sequence of the PH domain of AKT, with the C-terminus modified via the addition of a GFP tag. Cells were cultured on coverslips to approximately 90% confluence and transfected with 2 μg of AKT-PH-GFP construct using 6 μl of Lipofectamine 2000 (Invitrogen). At 24 hours post-transfection, the cells were transferred to 39°C or maintained at 34°C. 24 hours later, the cells were serum starved (0.5% FBS) overnight (~16 hours) and subsequently stimulated for 30-60 minutes, depending on the cells being studied, with 10% FBS or maintained in low-serum (0.5%) medium.

Coverslips were fixed in 4% formaldehyde for 30 minutes at 25°C, mounted on slides using gelvatol, and examined using a Zeiss Axiophot microscope with a digital camera and Northern Eclipse 6.0 image analyzer (Empix Imaging, Mississauga, ON, Canada). Three coverslips per condition were examined and the cells were counted, photographed and analyzed for AKT localization.

Proliferation/immunofluorescence

Cells were grown on coverslips to approximately 70% confluence and fixed in methanol at –20°C, permeabilized with 1:1 methanol:acetone for 5 minutes at –20°C, dried, washed and blocked with Dako protein block (Dako, Mississauga, Ontario, Canada) for 30 minutes. The coverslips were incubated overnight at 4°C with primary Ki-67 mouse anti-human mAb (Dako, #M0722) and in secondary Alexa-Fluor-594-labeled goat anti-mouse IgG (Cedarlane, Hornby, ON, Canada) for 1 hour at 25°C. At least six representative fields for each case were analyzed for Ki-67 staining.

Apoptosis

The cell death detection ELISA kit (Roche, Mississauga, ON, Canada) was used to detect histone complexes in apoptotic cells. At approximately 70% confluence, cells were moved to 39°C or maintained at 34°C and subsequently trypsinized, lysed and assay performed using the manufacturer's protocol at various time points. A microplate autoreader EL311 (Bio-TEK instruments, Winooski, VT) was used at 405 nm.

p53 adenovirus

Adenoviral constructs with wild-type p53 and with GFP were provided by Benjamin K. Tsang (University of Ottawa, ON, Canada) and synthesized by Ruth Slack (Adenovirus Core Facility, Neuroscience Research Institute, University of Ottawa,

Table 2. Non-tumorigenic cell lines: influence of wild-type TAg and ts TAg on the p53 status of the cells

Cell lines		TAg			p53 status	
			p53 binding			
Name	p53 genotype	Form	34°C	39°C	34°C	39°C
OSE	WT	N/A	N/A	N/A	Active	Active
WI38	WT	N/A	N/A	N/A	Active	Active
IOSE 397	WT	WT	+	+	Inactive	Inactive
IOSE 80pc	WT	WT	+	+	Inactive	Inactive
IOSE 166a	WT	ts	+	–	Inactive	Active
IOSE 166h	WT	ts	+	–	Inactive	Active
OSEC2	WT	ts	+	–	Inactive	Active

Cell lines: OSE, normal low-passage ovarian surface epithelium; WI38, representative control line with wild-type p53; IOSE, OSE transfected with either wild-type TAg (IOSE 397 and IOSE 80pc), ts TAg (IOSE 166a, 166h), or ts TAg plus human TERT (hTERT) (OSEC2). TAg, large T antigen; N/A, not applicable (not transfected with SV40TAg); +/–, binding to and inactivating p53/not binding to p53; ts, temperature sensitive; WT, wild type.

Journal of Cell Science

Journal of Cell Science

ON, Canada). This adenoviral wild-type p53 vector was constructed, purified and titered as described previously (Cregan et al., 2000). A panel of cancer cells were infected (multiplicity of infection = 20) with the adenoviral wild-type p53 and GFP control constructs. Adenovirus infection efficiency was >90%, as determined by GFP-construct-infected cells. 48 hours post infection, the cells were lysed for western blot analyses.

Bioinformatics

Promoter analysis was performed with annotations available in the University of California Santa Cruz (UCSC) genome browser (http://genome.ucsc.edu/). The annotations used include positions of exons defined by cDNA transcripts (including expressed sequence tags), cross-species sequence similarity based on genome sequence alignments (Karolchik et al., 2003) and CpG-island locations. The ConSite system (http://www.cisreg.ca/) and underlying ORCA alignment algorithm were used to identify evolutionary-conserved (mouse to human) regions on *PIK3CA* containing putative p53-binding sites. As described, the p53 consensus binding-site consists of two palindrome half-sites separated by 0-13 bp. The ConSite default search does not allow for variable spacing; therefore, half-site binding profiles were used to predict p53-binding sites. Based on the observation that bona fide p53 target sites often exhibit one half-site with a strong match to the consensus pattern and a second degenerate half-site, we screened the *PIK3CA* promoter sequence for such pairings within 0-13 bp. We applied two related profiles, with one containing a specific requirement at two positions within the core pattern (CnnG). The profiles are provided in supplementary material Fig. S1.

Rapid amplification of cDNA ends (5′ RACE)

Total RNA was isolated from cells with the RNeasy mini kit (Qiagen). 5′ RACE was performed with the 5′ RACE system kit (Invitrogen). A list of gene-specific primers (GSP) used is provided in supplementary material Table S2. GSP1 and GSP2 were designed to span regions of exon 3 and exon 2, and exon 2 and exon 1, respectively, in order to eliminate reverse transcription from genomic DNA. GSP3 was designed internal to exon 1 and was used for nested amplification of the primary PCR product.

Chromatin immunoprecipitation

ChIP was performed using the EZ-ChIP kit (Upstate, Charlottesville, VA). Cells were cultured at 80-90% confluency and chromatin harvested from cells at 39°C and 34°C were sheared with a 50-watt sonicator using 8×15-second pulses. A 100 μl aliquot of the sheared DNA was used for each immunoprecipitation. Mouse anti-IgG (1 μg) and anti-RNA polymerase II (1 μg) were used for immunoprecipitation of negative and positive controls, respectively. p53-bound chromatin segments were immunoprecipitated with 6 μg of anti-p53 monoclonal (1C12) mouse antibody (Cell Signaling Technologies catalog no. 2524). Moreover, primers (supplementary material Table S3) were designed around the putative p53-binding sites to give products between approximately 150 and 200 bp in length.

Electrophoretic mobility shift analysis

EMSA was performed using the LightShift Chemiluminescent EMSA kit (Pierce, Rockford, IL) as recommended by the manufacturer. For each reaction, 10 nM biotin-labeled double-stranded oligonucleotide (supplementary material Table S4) was incubated with nuclear lysates (6 μg total protein) or recombinant p53 (100 ng) (ProSpec-Tany TechnoGene, Rehovot, Israel) for 20 minutes at 25°C. Nuclear extracts were isolated using NE-PER nuclear and cytoplasmic extraction reagents (Pierce). Competition was demonstrated using unlabeled oligonucleotides. Supershift was performed by addition of p53 mouse monoclonal antibody (PAb421) (EMD Chemicals, San Diego, CA). Protein-DNA complexes were resolved by non-denaturing PAGE.

Reporter assay

PIK3CA promoter1a region was amplified by PCR using human genomic DNA. The luciferase reporter plasmid was constructed by subcloning *PIK3CA* promoter1a to *Kpn*I and *Xho*I sites in the pGL3-basic vector (Promega, Madison, WI). Point mutations were generated using site-directed mutagenesis. The dual luciferase reporter system (Promega) internally controlled with Renilla luciferase (phRL-TK) was used to measure activity of the *PIK3CA* promoter in OSEC2 at 39°C and 34°C. Cells were co-transfected with 1.5 μg of either *PIK3CA* promoter1a construct (pGL3-P1A), *PIK3CA* promoter1a construct mutated at site 4 (pGL3-P1A-mut4) within the specific core (CAAG conversion to AAAA), pGL3 control, or pGL3 basic and 0.5 μg of phRL-TK construct using 3 μl of Lipofectamine 2000 (Invitrogen). Cells were incubated overnight at 34°C then transferred to 39°C. After 24 hours, the cells were lysed with passive lysis buffer (Promega) for 45 minutes at 25°C while shaking. The Wallac VICTOR3 multilabel counter model 1420 was used to measure the luminescence.

This work was supported by a grant from the National Cancer Institute of Canada to N.A., National Institutes of Health grants PPG-PO1 CA64602 to G.B.M. and RO1 CA114017-01A1 to S.E.D., a Canadian Institutes of Health Research grant to W.W.W., and a studentship to A.A. by the Child and Family Research Institute, Vancouver B.C., Canada. We thank J. Y. Chou (National Institute of Child Health and Human Development, Bethesda, MD) for providing us with the ts-TAg construct and J. Q. Cheng (University of South Florida College of Medicine, Tampa, FL) for valuable discussions.

References

Arrick, B. A., Grendell, R. L. and Griffin, L. A. (1994). Enhanced translational efficiency of a novel transforming growth factor beta 3 mRNA in human breast cancer cells. *Mol. Cell. Biol.* **14**, 619-628.

Auersperg, N., Wong, A. S., Choi, K. C., Kang, S. K. and Leung, P. C. (2001). Ovarian surface epithelium: biology, endocrinology, and pathology. *Endocr. Rev.* **22**, 255-288.

Brown, C. Y., Mize, G. J., Pineda, M., George, D. L. and Morris, D. R. (1999). Role of two upstream open reading frames in the translational control of oncogene mdm2. *Oncogene* **18**, 5631-5637.

Brown, R., Clugston, C., Burns, P., Edlin, A., Vasey, P., Vojtesek, B. and Kaye, S. B. (1993). Increased accumulation of p53 protein in cisplatin-resistant ovarian cell lines. *Int. J. Cancer* **55**, 678-684.

Budhram-Mahadeo, V., Morris, P. J., Smith, M. D., Midgley, C. A., Boxer, L. M. and Latchman, D. S. (1999). p53 suppresses the activation of the Bcl-2 promoter by the Brn-3a POU family transcription factor. *J. Biol. Chem.* **274**, 15237-15244.

Chehab, N. H., Malikzay, A., Stavridi, E. S. and Halazonetis, T. D. (1999). Phosphorylation of Ser-20 mediates stabilization of human p53 in response to DNA damage. *Proc. Natl. Acad. Sci. USA* **96**, 13777-13782.

Chou, J. Y. (1989). Differentiated mammalian cell lines immortalized by temperature sensitive tumor viruses. *Mol. Endocrinol.* **3**, 1511-1514.

Cregan, S. P., MacLaurin, J., Gendron, T. F., Callaghan, S. M., Park, D. S., Parks, R. J., Graham, F. L., Morley, P. and Slack, R. S. (2000). Helper-dependent adenovirus vectors: their use as a gene delivery system to neurons. *Gene Ther.* **7**, 1200-1209.

Davies, B. R., Steele, I. A., Edmondson, R. J., Zwolinski, S. A., Saretzki, G., von Zglinicki, T. and O'Hare, M. J. (2003). Immortalisation of human ovarian surface epithelium with telomerase and temperature-sensitive SV40 large T antigen. *Exp. Cell Res.* **288**, 390-402.

Deligdisch, L., Einstein, A. J., Guera, D. and Gil, J. (1995). Ovarian dysplasia in epithelial inclusion cysts. A morphometric approach using neural networks. *Cancer* **76**, 1027-1034.

Duga, S., Asselta, R., Del Giacco, L., Malcovati, M., Ronchi, S., Tenchini, M. L. and Simonic, T. (1999). A new exon in the 5′ untranslated region of the connexin32 gene. *Eur. J. Biochem.* **259**, 188-196.

el-Deiry, W. S., Kern, S. E., Pietenpol, J. A., Kinzler, K. W. and Vogelstein, B. (1992). Definition of a consensus binding site for p53. *Nat. Genet.* **1**, 45-49.

Farmer, G., Colgan, J., Nakatani, Y., Manley, J. L. and Prives, C. (1996). Functional interaction between p53, the TATA-binding protein (TBP), andTBP-associated factors in vivo. *Mol. Cell. Biol.* **16**, 4295-4304.

Fraser, M., Leung, B., Jahani-Asl, A., Yan, X., Thompson, W. E. and Tsang, B. K. (2003a). Chemoresistance in human ovarian cancer: the role of apoptotic regulators. *Reprod. Biol. Endocrinol.* **1**, 66.

Fraser, M., Leung, B. M., Yan, X., Dan, H. C., Cheng, J. Q. and Tsang, B. K. (2003b). p53 is a determinant of X-linked inhibitor of apoptosis protein/Akt-mediated chemoresistance in human ovarian cancer cells. *Cancer Res.* **63**, 7081-7088.

Friedman, P. N., Chen, X., Bargonetti, J. and Prives, C. (1993). The p53 protein is an unusually shaped tetramer that binds directly to DNA. *Proc. Natl. Acad. Sci. USA* **90**, 3319-3323.

Gardiner-Garden, M. and Frommer, M. (1987). CpG islands in vertebrate genomes. *J. Mol. Biol.* **196**, 261-282.

Hempel, N., Wang, H., LeCluyse, E. L., McManus, M. E. and Negishi, M. (2004). The human sulfotransferase SULT1A1 gene is regulated in a synergistic manner by Sp1 and GA binding protein. *Mol. Pharmacol.* **66**, 1690-1701.

Hoffman, W. H., Biade, S., Zilfou, J. T., Chen, J. and Murphy, M. (2002). Transcriptional repression of the anti-apoptotic survivin gene by wild type p53. *J. Biol. Chem.* **277**, 3247-3257.

Hu, L., Zaloudek, C., Mills, G. B., Gray, J. and Jaffe, R. B. (2000). In vivo and in vitro ovarian carcinoma growth inhibition by a phosphatidylinositol 3-kinase inhibitor (LY294002). *Clin. Cancer Res.* **6**, 880-886.

Hu, L., Hofmann, J., Lu, Y., Mills, G. B. and Jaffe, R. B. (2002). Inhibition of phosphatidylinositol 3′-kinase increases efficacy of paclitaxel in in vitro and in vivo ovarian cancer models. *Cancer Res.* **62**, 1087-1092.

Iwabuchi, H., Sakamoto, M., Sakunaga, H., Ma, Y. Y., Carcangiu, M. L., Pinkel, D., Yang-Feng, T. L. and Gray, J. W. (1995). Genetic analysis of benign, low-grade, and high-grade ovarian tumors. *Cancer Res.* **55**, 6172-6180.

Johnson, R. A., Ince, T. A. and Scotto, K. W. (2001). Transcriptional repression by p53 through direct binding to a novel DNA element. *J. Biol. Chem.* **276**, 27716-27720.

Kanaya, T., Kyo, S., Hamada, K., Takakura, M., Kitagawa, Y., Harada, H. and Inoue, M. (2000). Adenoviral expression of p53 represses telomerase activity through down-regulation of human telomerase reverse transcriptase transcription. *Clin. Cancer Res.* **6**, 1239-1247.

Karolchik, D., Baertsch, R., Diekhans, M., Furey, T. S., Hinrichs, A., Lu, Y. T., Roskin, K. M., Schwartz, M., Sugnet, C. W., Thomas, D. J. et al. (2003). The UCSC genome browser database. *Nucleic Acids Res.* **31**, 51-54.

Kochetov, A. V., Ischenko, I. V., Vorobiev, D. G., Kel, A. E., Babenko, V. N., Kisselev, L. L. and Kolchanov, N. A. (1998). Eukaryotic mRNAs encoding abundant and scarce proteins are statistically dissimilar in many structural features. *FEBS Lett.* **440**, 351-355.

Kubbutat, M. H., Jones, S. N. and Vousden, K. H. (1997). Regulation of p53 stability by Mdm2. *Nature* **387**, 299-303.

Kupryjanczyk, J., Thor, A. D., Beauchamp, R., Merritt, V., Edgerton, S. M., Bell, D. A. and Yandell, D. W. (1993). p53 gene mutations and protein accumulation in human ovarian cancer. *Proc. Natl. Acad. Sci. USA* **90**, 4961-4965.

Lee, K. C., Crowe, A. J. and Barton, M. C. (1999). p53-mediated repression of alpha-fetoprotein gene expression by specific DNA binding. *Mol. Cell. Biol.* **19**, 1279-1288.

Lengauer, C., Kinzler, K. W. and Vogelstein, B. (1998). Genetic instabilities in human cancers. *Nature* **396**, 643-649.

Leung, E. H., Leung, P. C. and Auersperg, N. (2001). Differentiation and growth potential of human ovarian surface epithelial cells expressing temperature-sensitive SV40 T antigen. *In Vitro Cell. Dev. Biol. Anim.* **37**, 515-521.

Levine, D. A., Bogomolniy, F., Yee, C. J., Lash, A., Barakat, R. R., Borgen, P. I. and Boyd, J. (2005). Frequent mutation of the PIK3CA gene in ovarian and breast cancers. *Clin. Cancer Res.* **11**, 2875-2878.

Maines-Bandiera, S. L., Kruk, P. A. and Auersperg, N. (1992). Simian virus 40-transformed human ovarian surface epithelial cells escape normal growth controls but retain morphogenetic responses to extracellular matrix. *Am. J. Obstet. Gynecol.* **167**, 729-735.

May, P. and May, E. (1999). Twenty years of p53 research: structural and functional aspects of the p53 protein. *Oncogene* **18**, 7621-7636.

Mayo, L. D. and Donner, D. B. (2001). A phosphatidylinositol 3-kinase/Akt pathway promotes translocation of Mdm2 from the cytoplasm to the nucleus. *Proc. Natl. Acad. Sci. USA* **98**, 11598-11603.

McLure, K. G. and Lee, P. W. (1998). How p53 binds DNA as a tetramer. *EMBO J.* **17**, 3342-3350.

Meric, F. and Hunt, K. K. (2002). Translation initiation in cancer: a novel target for therapy. *Mol. Cancer Ther.* **1**, 971-979.

Obata, K., Morland, S. J., Watson, R. H., Hitchcock, A., Chenevix-Trench, G., Thomas, E. J. and Campbell, I. G. (1998). Frequent PTEN/MMAC mutations in endometrioid but not serous or mucinous epithelial ovarian tumors. *Cancer Res.* **58**, 2095-2097.

O'Brate, A. and Giannakakou, P. (2003). The importance of p53 location: nuclear or cytoplasmic zip code? *Drug Resist. Updat.* **6**, 313-322.

O'Connor, P. M., Jackman, J., Bae, I., Myers, T. G., Fan, S., Mutoh, M., Scudiero, D. A., Monks, A., Sausville, E. A., Weinstein, J. N. et al. (1997). Characterization of the p53 tumor suppressor pathway in cell lines of the National Cancer Institute anticancer drug screen and correlations with the growth-inhibitory potency of 123 anticancer agents. *Cancer Res.* **57**, 4285-4300.

Pipas, J. M. and Levine, A. J. (2001). Role of T antigen interactions with p53 in tumorigenesis. *Semin. Cancer Biol.* **11**, 23-30.

Sabbatini, P. and McCormick, F. (1999). Phosphoinositide 3-OH kinase (PI3K) and PKB/Akt delay the onset of p53-mediated, transcriptionally dependent apoptosis. *J. Biol. Chem.* **274**, 24263-24269.

Samuels, Y. and Velculescu, V. E. (2004). Oncogenic mutations of PIK3CA in human cancers. *Cell Cycle* **3**, 1221-1224.

Savitsky, K., Platzer, M., Uziel, T., Gilad, S., Sartiel, A., Rosenthal, A., Elroy-Stein, O., Shiloh, Y. and Rotman, G. (1997). Ataxia-telangiectasia: structural diversity of untranslated sequences suggests complex post-transcriptional regulation of ATM gene expression. *Nucleic Acids Res.* **25**, 1678-1684.

Schlosshauer, P. W., Cohen, C. J., Penault-Llorca, F., Miranda, C. R., Bignon, Y. J., Dauplat, J. and Deligdisch, L. (2003). Prophylactic oophorectomy: a morphologic and immunohistochemical study. *Cancer* **98**, 2599-2606.

Seto, E., Usheva, A., Zambetti, G. P., Momand, J., Horikoshi, N., Weinmann, R., Levine, A. J. and Shenk, T. (1992). Wild-type p53 binds to the TATA-binding protein and represses transcription. *Proc. Natl. Acad. Sci. USA* **89**, 12028-12032.

Shayesteh, L., Lu, Y., Kuo, W. L., Baldocchi, R., Godfrey, T., Collins, C., Pinkel, D., Powell, B., Mills, G. B. and Gray, J. W. (1999). PIK3CA is implicated as an oncogene in ovarian cancer. *Nat. Genet.* **21**, 99-102.

Shieh, S. Y., Taya, Y. and Prives, C. (1999). DNA damage-inducible phosphorylation of p53 at N-terminal sites including a novel site, Ser20, requires tetramerization. *EMBO J.* **18**, 1815-1823.

Singh, B., Reddy, P. G., Goberdhan, A., Walsh, C., Dao, S., Ngai, I., Chou, T. C., O-charoenrat, P., Levine, A. J., Rao, P. H. et al. (2002). p53 regulates cell survival by inhibiting PIK3CA in squamous cell carcinomas. *Genes Dev.* **16**, 984-993.

Sobczak, K. and Krzyzosiak, W. J. (2002). Structural determinants of BRCA1 translational regulation. *J. Biol. Chem.* **277**, 17349-17358.

Stambolic, V., MacPherson, D., Sas, D., Lin, Y., Snow, B., Jang, Y., Benchimol, S. and Mak, T. W. (2001). Regulation of PTEN transcription by p53. *Mol. Cell* **8**, 317-325.

Subbaramaiah, K., Altorki, N., Chung, W. J., Mestre, J. R., Sampat, A. and Dannenberg, A. J. (1999). Inhibition of cyclooxygenase-2 gene expression by p53. *J. Biol. Chem.* **274**, 10911-10915.

Sun, Y., Wenger, L., Rutter, J. L., Brinckerhoff, C. E. and Cheung, H. S. (1999). p53 down-regulates human matrix metalloproteinase-1 (Collagenase-1) gene expression. *J. Biol. Chem.* **274**, 11535-11540.

Suzuki, S., Moore, D. H., 2nd, Ginzinger, D. G., Godfrey, T. E., Barclay, J., Powell, B., Pinkel, D., Zaloudek, C., Lu, K., Mills, G. et al. (2000). An approach to analysis of large-scale correlations between genome changes and clinical endpoints in ovarian cancer. *Cancer Res.* **60**, 5382-5385.

Takahashi, K., Sumimoto, H., Suzuki, K. and Ono, T. (1993). Protein synthesis-dependent cytoplasmic translocation of p53 protein after serum stimulation of growth-arrested MCF-7 cells. *Mol. Carcinog.* **8**, 58-66.

Toker, A. and Cantley, L. C. (1997). Signalling through the lipid products of phosphoinositide-3-OH kinase. *Nature* **387**, 673-676.

Truant, R., Xiao, H., Ingles, C. J. and Greenblatt, J. (1993). Direct interaction between the transcriptional activation domain of human p53 and the TATA box-binding protein. *J. Biol. Chem.* **268**, 2284-2287.

Unger, T., Juven-Gershon, T., Moallem, E., Berger, M., Vogt Sionov, R., Lozano, G., Oren, M. and Haupt, Y. (1999). Critical role for Ser20 of human p53 in the negative regulation of p53 by Mdm2. *EMBO J.* **18**, 1805-1814.

Wang, Y., Helland, A., Holm, R., Kristensen, G. B. and Borresen-Dale, A. L. (2005). PIK3CA mutations in advanced ovarian carcinomas. *Hum. Mutat.* **25**, 322.

Xu, C. F., Chambers, J. A., Nicolai, H., Brown, M. A., Hujeirat, Y., Mohammed, S., Hodgson, S., Kelsell, D. P., Spurr, N. K., Bishop, D. T. et al. (1997). Mutations and alternative splicing of the BRCA1 gene in UK breast/ovarian cancer families. *Genes Chromosomes Cancer* **18**, 102-110.

Yaginuma, Y. and Westphal, H. (1992). Abnormal structure and expression of the p53 gene in human ovarian carcinoma cell lines. *Cancer Res.* **52**, 4196-4199.

Yuan, Z. Q., Feldman, R. I., Sussman, G. E., Coppola, D., Nicosia, S. V. and Cheng, J. Q. (2003). AKT2 inhibition of cisplatin-induced JNK/p38 and Bax activation by phosphorylation of ASK1: implication of AKT2 in chemoresistance. *J. Biol. Chem.* **278**, 23432-23440.

Zhou, B. P., Liao, Y., Xia, W., Zou, Y., Spohn, B. and Hung, M. C. (2001). HER-2/neu induces p53 ubiquitination via Akt-mediated MDM2 phosphorylation. *Nat. Cell Biol.* **3**, 973-982.

Journal of Cell Science